Available online at www.sciencedirect.com
SCIENCE DIRECT®
International Journal of Thermal Sciences 42 (2003) 837–846
International Journal of Thermal Sciences
www.elsevier.com/locate/ijts

Experimental analysis of asymmetrical isoflux channel-chimney systems

Oronzio Manca [a], Marilena Musto [a], Vincenzo Naso [b,*]

[a] *DIAM – Dipartimento di Ingegneria Aerospaziale e Meccanica, Seconda Università degli studi di Napoli, Real Casa dell'Annunziata, Via Roma, 29-81031 Aversa (CE), Italy*
[b] *DETEC – Dipartimento di Energetica, Termofluidodinamica applicata e Condizionamenti ambientali, Università degli studi di Napoli Federico II, Piazzale Tecchio, 80-80125 Napoli, Italy*

Received 13 May 2002; accepted 13 May 2002

Abstract

Air natural convection in an asymmetrically heated channel with unheated extensions has been investigated experimentally. Local and maximum wall temperatures and heat transfer coefficients are presented, for different values of the process parameters. Optimal configurations in terms of the minimum values of maximum wall temperatures are obtained. Average Nusselt numbers and maximum dimensionless wall temperatures are correlated to the Rayleigh number and to the geometrical dimensionless parameters in the $10–1.5 \times 10^5$ range of the Rayleigh number times the expansion ratio. The addition of downstream unheated extensions improves the thermal performance of the channel for some configurations, the longer the extension and the lower the aspect ratio the lower the wall temperature in the channel.

Keywords: Natural convection; Channel-chimney system; Vertical channel; Uniform heat flux; Experimental investigation; Correlation; Electronics cooling

1. Introduction

Because of the continuously increasing heat rate dissipated in electronic systems the maximum temperature of the components could attain such a value as to jeopardize the system performance and reliability. A suitable thermal control of electronic components can guarantee that the operating temperature does not exceed the prescribed threshold. In many applications it is advantageous to employ natural convection, since it is cheap, maintenance and noise free and reliable [1]. One of the more frequently investigated configurations is the vertical channel [2]. Uniformly heated channels, both symmetrically and asymmetrically, have been widely studied [3–5]. The heat rate transferred by natural convection in a vertical channel can be enhanced by providing the heated channel with unheated extensions downstream of its heated walls [6,7]. The increase in the heat transfer rate is obtained by means of the chimney effect, which is also used for heat sink configurations such as those shown in [8–11]. Similarly, it is of interest to find out geometric arrangements which allow the thermal optimization of the control system, as it was shown for natural convection in [12], and more optimized configurations were reviewed in [13]. As far as systems with downstream adiabatic extensions are concerned, the process parameters include the extension ratio, associated with the height of the adiabatic extension, and the expansion ratio, related to the distance between the unheated extensions.

A review of the studies on natural convection in a vertical channel with downstream adiabatic extensions is reported in the following. The channel-chimney system was investigated both experimentally and numerically in [6,7,14, 15]. Haaland and Sparrow [14] for the first time in a numerical study showed that adding adiabatic walls downstream of a channel with a point heat source or distributed heat sources determined an increase in the flow rate. The effects of adiabatic extensions coplanar to the walls of a symmetrically heated vertical channel were analyzed only numerically in [16,17]. Oosthuizen [16] investigated a symmetrically heated channel with uniform wall temperature. Results showed that significant increases in heat transfer rate were obtained only with very long adiabatic extensions downstream of the heated channel. The effects of an unheated entry or unheated exit region on natural convection in vertical channels with isotherm or isoflux walls were investigated numerically [17]. The unheated entry or unheated exit

* Corresponding author.
E-mail addresses: manca@unina.it (O. Manca), milenamusto@libero.it (M. Musto), vinaso@unina.it (V. Naso).

1290-0729/$ – see front matter
doi:10.1016/S1290-0729(03)00056-5

Nomenclature

b	channel spacing	m
B	extension spacing	m
B/b	expansion ratio	
g	acceleration of gravity	$m{\cdot}s^{-2}$
Gr	channel Grashof number, Eq. (2)	
k	thermal conductivity	$W{\cdot}m^{-1}{\cdot}K^{-1}$
L	overall length	m
L/L_h	extension ratio	
L_h/b	channel aspect ratio	
L_h	channel length	m
L_{ext}	extension length	m
m', n'	coefficients in Eq. (10)	
m'', n''	coefficients in Eq. (13)	
Nu	channel Nusselt number, Eq. (4)	
Pr	Prandtl number	
q	heat flux	$W{\cdot}m^{-2}$
r	regression coefficient	
Ra^*	channel Rayleigh number, Eq. (2)	
T	temperature	K
T^*	dimensionless temperature, Eq. (6)	
x, y, z	coordinates	m
X	dimensionless coordinate, Eq. (1)	

Greek symbols

β	volumetric coefficient of expansion	K^{-1}
ν	kinematic viscosity	$m^2{\cdot}s^{-1}$

Subscripts

c	convective
k	conductive
max	maximum
max, 0	maximum, refers to *base case*
o	ambient air
r	radiative
w	wall
Ω	Ohmic dissipation

section affects the natural convection in the channel, particularly at low Rayleigh numbers. A strong influence on natural convection at high Rayleigh number was observed in channels with uniform heat flux at the walls and with an unheated exit region. The numerical analysis of an isoflux heated channel with a downstream adiabatic extension was carried out in [18]. A reduction of the maximum wall temperature was found and the larger the Rayleigh number the less the reduction. The influence of width of the gap between the adiabatic extensions was also investigated [6,7,15, 16]. A numerical study of a vertical isothermal tube with an unheated extension was carried out by Asako et al. [19]. Optimal configurations, which maximize the heat transfer rate, were derived. A numerical and experimental investigation on vertical isothermal channels with adiabatic extensions was carried out by Straatman et al. [6]. The increase in heat transfer rates was larger at low Rayleigh numbers than at high Rayleigh numbers. A single correlation among Nusselt number, channel Rayleigh number and geometric parameters was proposed. A system made of isothermal multiple vertical channels (periodic channel expanded chimney) was numerically analyzed in [15]. The interaction between multiple channels increased the flow rate and the associated chimney effect was stronger than in a single channel with adiabatic extensions. A system with the symmetrically heated channel at uniform wall heat flux was studied experimentally by Auletta et al. [7], where results were derived in terms of geometric parameters and Rayleigh numbers; correlations for dimensionless maximum temperature and Nusselt numbers in terms of channel Rayleigh number and geometrical parameters were presented.

To the authors' knowledge the thermal analysis of natural convection in a chimney-channel, asymmetrically heated with a uniform wall heat flux, has not yet been carried out. Results of an experimental investigation on the aforementioned system are presented in this paper. The study was carried out, according to the procedure presented by Auletta et al. [7], for an asymmetrically heated channel with unheated extensions. Current and maximum wall temperatures and heat transfer coefficients are presented, for different values of the process parameters. Optimal configurations in terms of the minimum values of maximum wall temperatures are obtained. Average Nusselt numbers and maximum dimensionless wall temperatures in the $10–1.5 \times 10^5$ range of the Rayleigh number times the expansion ratio are presented. They are correlated to the Rayleigh number and to the geometrical dimensionless parameters.

2. Experimental apparatus

A sketch of the channel-chimney system under investigation is shown in Fig. 1(a). The axial coordinate and that along the channel gap are indicated with x and y, respectively. The transverse axis z, orthogonal to the picture plane, is not shown in the figure. The configuration was made of two vertical walls (channel), one heated and one unheated, and of two downstream unheated parallel extensions (chimney). The channel walls were made of a 3.2 mm thick and 530 mm wide phenolic fiberboard plate, with a typical thermal conductivity of 0.17 $W{\cdot}m^{-1}{\cdot}K^{-1}$. Their surface facing the channel was coated with a 16 μm thick copper layer, which was the heater. Heat losses from the back of each wall of the channel were reduced by sticking a 120 mm polystyrene block on the rear surface of each wall. The cross-section of the heated wall is sketched in Fig. 1(b).

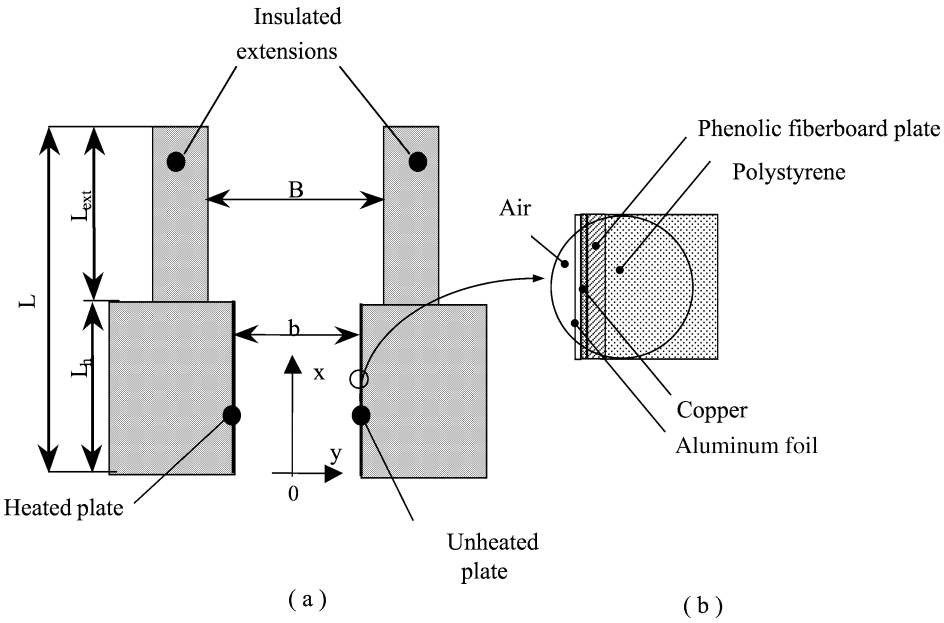

Fig. 1. Sketch of the experimental apparatus: (a) test section; (b) heated wall.

The heater was obtained by cutting the copper layer in a 4.6 mm wide and 9.0 m long serpentine track. Its expected electric resistance was about 0.50 Ω. The electric supply wire was soldered to a thick copper bar bolted to the ends of the heater. No electric resistance between the heater and the bars was measured during preliminary tests. The dissipated heat rate through the electrical resistance was evaluated with an accuracy of ±2 percent, by measuring the voltage drop and the direct current. The chimney was made of two 30 mm thick and 530 mm wide polystyrene blocks. A self-adhesive 25 μm thick aluminum foil was stuck on the surfaces facing the channel and the chimney to obtain a low emissivity of the walls. A 0.1 value of the total emissivity was evaluated, by means of a radiometric direct measurement.

A suitable electric insulation between the copper surfaces and the aluminum foil was assured by uniformly spraying an electrically insulating varnish onto them before coating. Side walls of the channel-chimney system were made of Plexiglas rectangular rods placed between the walls at their lateral edges. The rods were machined within an accuracy of ±0.025 mm and the gap of the adiabatic extensions was measured with an accuracy of ±0.50 mm. The channel-chimney system was opened to the ambient only along the top and the bottom edges. The walls were fastened together by a steel frame, which was designed in such a way as not to obstruct the fluid flow in the proximity of the channel inlet. The channel and the chimney were aligned vertically, with horizontal leading edges, by means of a plumb line and a level. The clearance of the bottom edges of the heated walls above the floor was 1.20 m and the minimum distance between the exit section of the chimney and the ceiling was 1.80 m.

The entire apparatus was located in an enclosed room, accurately sealed in order to eliminate extraneous air current and air drafts were further reduced by a 2.5 m high vertical screen. A large fraction of the lower part of the screen was made up by a 0.20 m high mesh. The measured differences in the ambient air temperature in the proximity of the inlet and the exit sections of the apparatus were less than 0.8 K. The channel-chimney system was 475 mm wide. The length of the channel was $L_h = 100$ mm, and that of the chimney, L_{ext}, varied in the 0–300 mm range. The channel spacing, b, varied in the 5.0–20.0 mm range; that of the chimney, B, varied in the 5.0–80.0 mm range. With this dimensions, the channel aspect ratio L_h/b was in the 5.0–20.0 range and the expansion ratio B/b ranged between 1.0 and 4.0.

Wall temperatures were measured by 0.50 mm OD copper-constantan thermocouples (type T), embedded in the fiberboard in the very proximity of the back side of the copper layer and bonded with a 3M epoxy glue. Thermocouples were run horizontally, parallel to the surfaces, thereby lying along isotherms in order minimize conduction heat losses in the leads. Ten equally spaced thermocouples were placed in the centerline of the heated plate: the first was placed 5.0 mm downstream of the inlet section, the distance between two successive thermocouples being 10 mm. At 75 mm from the leading edge of the walls, eight additional thermocouples were located horizontally outward from the centerline at $z = \pm 100$ mm, ±125 mm and ±150 mm in order to provide indications of the horizontal variation in the wall temperature. The ambient air temperature was measured by the same type of thermocouples located in the proximity of the leading edge of the channel. Fifteen thermocouples were affixed to the rear surface of the plates and embedded in the polystyrene block, in order to evaluate the conductive heat losses.

Thermocouples voltages were recorded to 1 μV. Each thermocouple was calibrated in a 0.01 K thermostatic bath

by means of a reference standard thermometer (Pt 100). The calibration of the temperature measuring system showed an estimated precision of the thermocouple-readout system of ±0.1 K. A National Instrument SCXI module data acquisition system and a personal computer were used for the data collection and reduction. The data acquisition was performed through the LabView^{TM} software.

Tests showed that the wall temperature in the heated plate at the same x location can be assumed to be symmetric, the differences being within ±0.2 °C. Wall temperature was assumed to be independent of the z coordinate within $z = \pm 100$ mm, since in this region its maximum deviation from the centerline temperature was found to be no larger than 1.0 °C when the latter was 70.0 °C. No fluctuations in the wall temperature were measured during the tests. The typical time interval to attain steady-state conditions after modifying the electric power supply was nearly 3 hours.

3. Data reduction

With reference to Fig. 1(a), the main geometrical parameters used in this investigation are the channel aspect ratio, L_h/b, the expansion ratio, B/b, and the extension ratio, L/L_h.

The dimensionless coordinate along the length is

$$X = \frac{x}{L_h} \tag{1}$$

The channel Rayleigh number is defined as

$$Ra^* = Gr\frac{b}{L_h}Pr = \frac{g\beta q_c b^4}{\nu^2 k}\frac{b}{L_h}Pr \tag{2}$$

where q_c is the spatially-averaged convective heat flux on the heated wall

$$q_c = \frac{1}{L_h}\int_0^{L_h} q_c(x)\,dx \tag{3}$$

The channel Nusselt number is based on the difference between the wall and the inlet fluid temperatures, rather than on that between the wall and the bulk fluid temperatures, since the last one cannot be easily measured in practical applications

$$Nu = \frac{q_c b}{(T_w - T_o)k} \tag{4}$$

with the average wall temperature, T_w, defined as

$$T_w = \frac{1}{2L_h}\int_0^{L_h} T_w(x)\,dx \tag{5}$$

where $T_w(x)$ is the local temperature of the heated wall.

The dimensionless wall temperature is

$$T_w^* = \frac{(T_w - T_o)k}{q_c b} \tag{6}$$

The properties of the air are evaluated at the reference temperature $(T_w + T_o)/2$.

The local convective heat flux, $q_c(x)$, is not uniform because of radiation and conduction. Experimental data are reduced by first introducing, in the equations presented above, the local convective heat flux

$$q_c(x) = q_\Omega(x) - q_k(x) - q_r(x) \tag{7}$$

In Eq. (7) the overall heat rate divided by the area of the heated wall surface is the local heat flux due to Ohmic dissipation, $q_\Omega(x)$, which was assumed to be uniform along the heated plate; $q_k(x)$ denotes the local conduction heat losses from the plates and $q_r(x)$ is the local radiative heat flux from the plates. For each run, the terms $q_k(x)$ were calculated by a finite difference numerical procedure, a three-dimensional distribution of the temperature being assumed in the polystyrene. The predicted temperatures in significant configurations of the system had been previously compared to those measured by the thermocouples embedded in the polystyrene insulation and the agreement was very good, the maximum deviation being 4 percent. The $q_r(x)$ terms were calculated, for each temperature distribution in the walls, ambient temperature and channel spacing, by dividing each plate into sixteen strips along its length, according to the procedure described by Webb and Hill [5]. A two-dimensional radiative cavity was considered, which was made of the two plates, assumed as diffuse-gray surfaces, and the two edge sections, assumed as black at ambient temperature. In all the investigated configurations the conductive heat losses were about 9 percent of the Ohmic wall heat flux and the radiative heat losses ranged between about 3 percent and 5 percent.

4. Uncertainty analysis

The uncertainty in the calculated quantities was determined in conformity to the standard single sample analysis recommended by Kline and McClintock [20] and Moffat [21]. Accordingly, the uncertainty of a dependent variable R as a function of the uncertainties in the independent variables X_i is given by the relation

$$\delta R = \left[\left(\frac{\partial R}{\partial X_1}\delta X_1\right)^2 + \left(\frac{\partial R}{\partial X_2}\delta X_2\right)^2 + \cdots + \left(\frac{\partial R}{\partial X_n}\delta X_n\right)^2\right]^{1/2} \tag{8}$$

The uncertainty in the values of the air thermophysical properties can be assumed to be negligible. On the basis of Eqs. (2), (4), (6), (7) and of the maximum percent uncertainties in the values of the independent variables, which are reported in Table 1, the maximum uncertainty in Ra^* ranged from 5 percent to 8 percent whereas the maximum uncertainty in Nu and in $T^*_{w,max}$ turned out to be 4 percent to 7 percent.

Table 1
Maximum percent uncertainty values ($(\delta X_i / X_i) \times 100$)

Variable	T_w	T_o	$T_w - T_o$	b	q_c	q_r	q_Ω	q_k
Uncertainty	0.50	0.93	1.1	1.2	3.0	5.0	2.0	4.0

5. Results and discussion

Experiments were carried out on configurations of the system with $q_\Omega = 100, 300$ and 450 W·m^{-2}, $L_h/b = 5.0$, 10.0 and 20.0, $L/L_h = 1.0$, 2.0, 3.0 and 4.0, B/b ranging between 1.0 and 4.0. The channel Rayleigh number times the expansion ratio, $Ra^* \times B/b$, was in the range 10–1.5×10^5. The configuration with $L/L_h = 1.0$ is the channel without insulated extensions, which in the following will be referred to as *base case*. It should be taken in mind that the configuration with $B/b \to \infty$ physically coincides with the *base case* ($L/L_h = 1.0$).

5.1. Wall temperatures

The temperature rise of the heated wall above the ambient temperature as a function of the dimensionless axial coordinate, for $L_h/b = 20.0$, $q_\Omega = 100$ W·m^{-2} and different values of B/b and of L/L_h, is reported in Fig. 2. In all cases the maximum wall temperature is not attained in the exit section of the channel, because of the radiative edge effects to the ambient, the heat conduction to the polystyrene and the thermal plume in the exit section of the heated plate. Both figures exhibit very similar wall temperature patterns at all expansion ratios. In Fig. 2(a) one can remark that the lowest wall temperatures are attained for $B/b = 3.0$ and the highest are those for $B/b = 1.0$. This likely occurs because the larger the expansion ratio, and the cross section of the chimney, the smaller the pressure drop in it. For the configuration under investigation, at the largest value of the chimney gap ($B/b = 4.0$) adding the unheated extension practically does not enhance the thermal performance of the channel. Fig. 2(b) shows that adding a longer chimney to the channel ($L/L_h = 4.0$) improves its performance at any expansion ratios except for $B/b = 1.0$; the optimum configuration among those which have been investigated is that with $B/b = 4.0$.

Wall temperature rise above the ambient temperature as a function of the dimensionless axial coordinate, for $L_h/b = 10.0$, $q_\Omega = 100$ W·m^{-2} and different values of B/b and of L/L_h, is reported in Fig. 3. Comparing results in Figs. 3 and 2, we can notice that wall temperatures are lower in the channel twice larger than the other, all other process parameters being the same. This is due to the easier entrainment of air flow which, on turn, enhances convective heat transfer. Fig. 3(a) shows that adding a chimney as long as the heated channel is worthless, apart from the case of an expansion ratio $B/b = 2.0$. On the contrary, in Fig. 3(b) we can remark that the addition of a longer chimney improves the thermal performance of the system for all configurations apart from that with $B/b = 1.0$, thanks to the increase in the driving force caused by the chimney as well as to its width which determines a pressure recovery in the chimney and a pressure drop in the exit region of the heated channel.

Wall temperature rise above the ambient temperature as a function of the dimensionless axial coordinate, for $L_h/b = 5.0$, $q_\Omega = 100$ W·m^{-2} and different values of B/b and of L/L_h, is reported in Fig. 4. One can clearly notice that for the lowest aspect ratio and the larger extension ratio (Fig. 4(b)), whichever the expansion ratio, wall temperatures in a channel with the adiabatic extension are far lower than those in the channel without it. Comparing results in Figs. 2, 3 and 4 we can conclude that with $L/L_h = 4.0$, all other parameters being the same, the larger the system the lower the wall temperatures, since the increasing channel gap practically does not affect both the air inflow from the upper exit section of the system and the thermal plume, which drives a larger mass flow rate in the wider channel.

Wall temperature rise above the ambient temperature as a function of the dimensionless axial coordinate, for $L_h/b = 10.0$, $q_\Omega = 450$ W·m^{-2} and different values of B/b and of L/L_h, is reported in Fig. 5. As already noticed in Fig. 3(a) for a far lower dissipated heat flux all other quantities being the same, Fig. 5(a) shows that the addition of unheated extensions slightly lowers the wall temperature only when the expansion ratio is $B/b = 2.0$, probably thanks

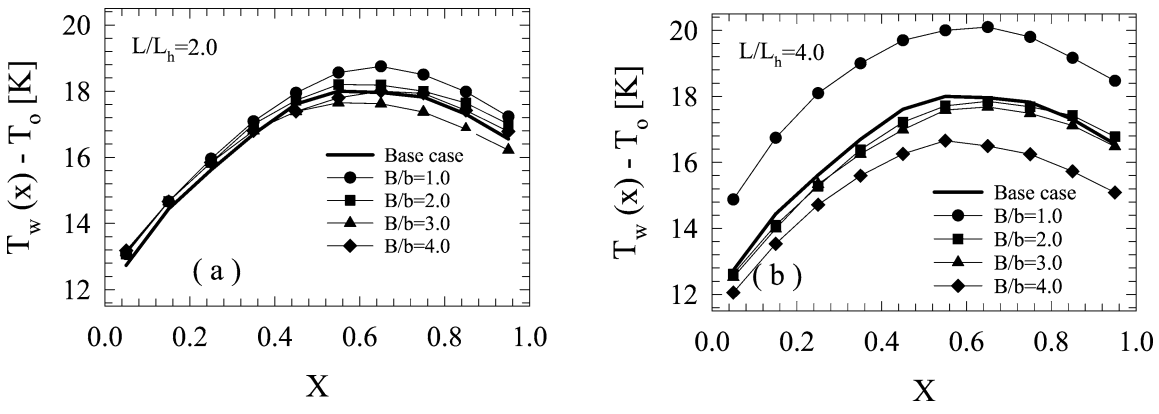

Fig. 2. Wall temperature rise vs the axial coordinate, for $L_h/b = 20.0$, $q_\Omega = 100$ W·m^{-2} and various B/b: (a) $L/L_h = 2.0$; (b) $L/L_h = 4.0$.

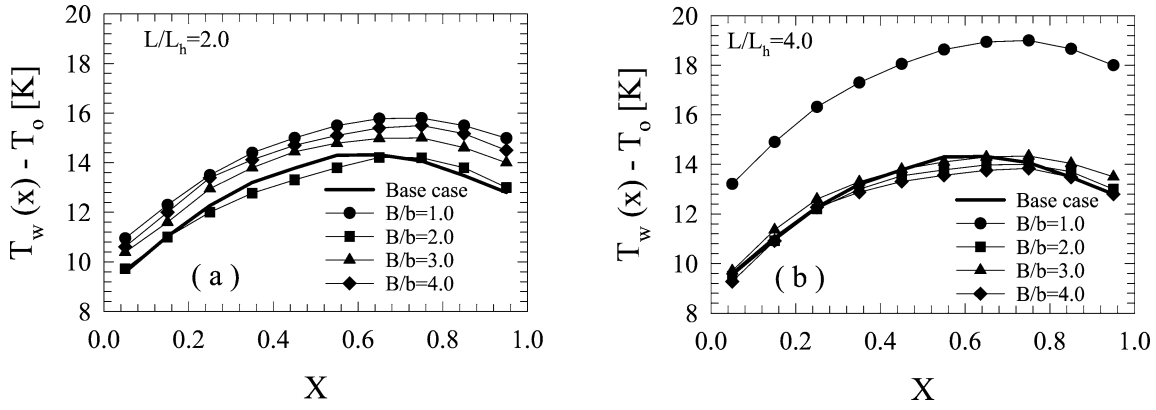

Fig. 3. Wall temperature rise vs the axial coordinate, for $L_h/b = 10.0$, $q_\Omega = 100$ W·m^{-2} and various B/b: (a) $L/L_h = 2.0$; (b) $L/L_h = 4.0$.

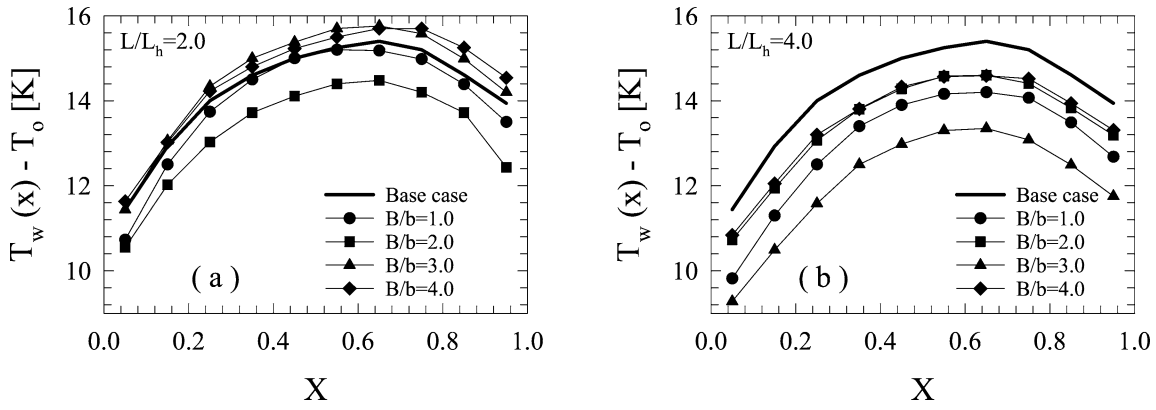

Fig. 4. Wall temperature rise vs the axial coordinate, for $L_h/b = 5.0$, $q_\Omega = 100$ W·m^{-2} and various B/b: (a) $L/L_h = 2.0$; (b) $L/L_h = 4.0$.

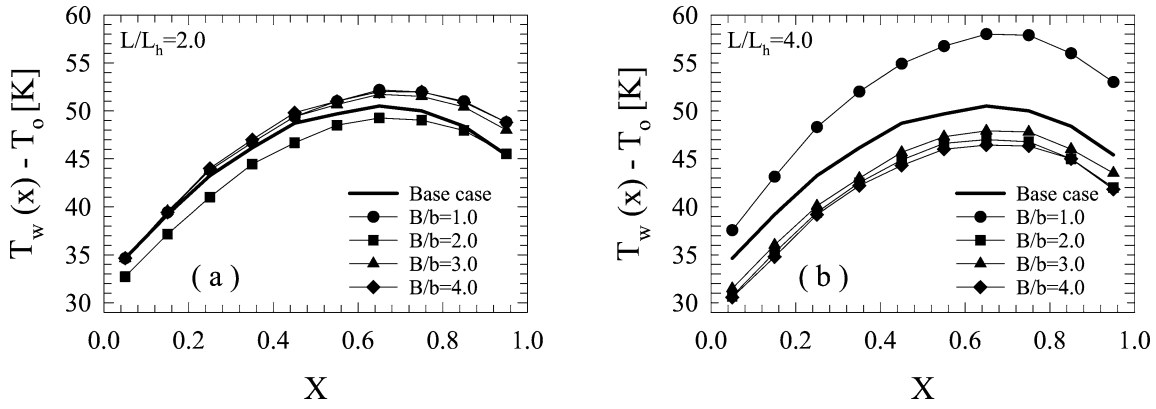

Fig. 5. Wall temperature rise vs the axial coordinate, for $L_h/b = 10.0$, $q_\Omega = 450$ W·m^{-2} and various B/b: (a) $L/L_h = 2.0$; (b) $L/L_h = 4.0$.

to a thinner boundary layer which weakens the effects of the ambient air downflow into the system. On the contrary, Fig. 5(b) shows that, in a larger channel ($L/L_h = 4.0$), except for $B/b = 1.0$, at any expansion ratios adding the chimney lowers the wall temperature.

Wall temperature rise above the ambient temperature as a function of the dimensionless axial coordinate, for $L_h/b = 5.0$, $q_\Omega = 450$ W·m^{-2} and different values of B/b and of L/L_h, is reported in Fig. 6. We can remark that in this configuration wall temperature is weakly affected by the expansion ratio at both L/L_h values, particularly in the hottest region of the wall. Moreover, Fig. 6 shows that adding adiabatic extension to the heated channel is worthwhile only if $L/L_h = 4.0$, like it was already pointed out observing data in Fig. 4(b). Because of the curves clustering an optimum value of the expansion ratio cannot be identified.

The ratio of the maximum temperature rise of the heated wall above the ambient air in a channel with the adiabatic extension to the one in a channel without the adiabatic extension as a function of the expansion ratio for different values of the extension ratio and of the wall heat flux, at channel aspect ratios equal to 5.0, 10.0 and 20.0, is reported

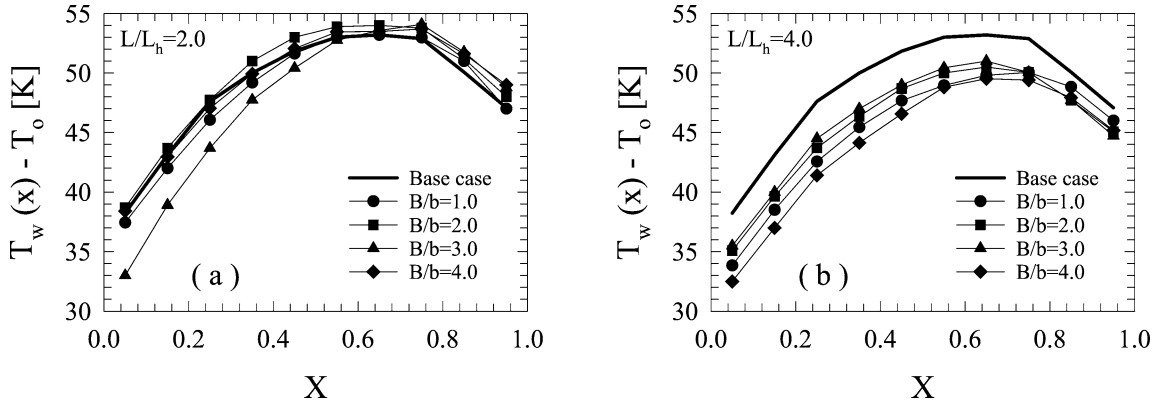

Fig. 6. Wall temperature rise vs the axial coordinate, for $L_h/b = 5.0$, $q_\Omega = 450$ W·m^{-2} and various B/b: (a) $L/L_h = 2.0$; (b) $L/L_h = 4.0$.

in Figs. 7, 8 and 9, respectively. They point out the effect of the unheated extension on the thermal performance of the system, with reference to the maximum wall temperature and allow to identify the optimum configurations. Fig. 7 shows similar thermal patterns of $\Delta T_{max}/\Delta T_{max,o}$ at $L_h/b = 5.0$, whichever the extension ratio, L/L_h, and the heat flux, all the values of the maximum wall temperature ratio laying in a ±15 percent range. The best performing thermal configurations are those with an expansion ratio B/b equal to 1.0 or 2.0.

Data in Fig. 8 show that at a larger value of the channel aspect ratio ($L_h/b = 10.0$) the best thermal performance of the channel with long adiabatic extensions ($L/L_h = 4.0$) is generally obtained with $B/b = 3.0$ and 4.0. On the contrary, when the chimney is as large as the channel ($B/b = 1.0$) the chimney-channel system performs worst than the simple channel, likely because of the strong pressure drop.

Similar observations can be made by observing results in Fig. 9, for the narrowest channel ($L_h/b = 20$), where in almost all cases maximum wall temperatures in a chimney-channel system are higher than those in a simple channel.

In the investigated field of the process parameters the configuration with a chimney four times longer than the channel ($L/L_h = 4.0$) exhibited the best performance, whichever the values of the other parameters. As a matter of fact, when the unheated extension is long enough the ambient air downflow in the chimney is prevented from reaching the exit cross section of the channel and, as a consequence, the thermal plume arising from its heated wall is not chocked.

5.2. Correlations for maximum wall temperatures

According to the analysis carried out by Straatman et al. [6], the dimensionless maximum wall temperature was correlated to the channel Rayleigh number times the expansion ratio, in the 10–1.5 × 10^5 range of $Ra^* \times B/b$, and to the extension ratio, in the 2.0–4.0 range of L/L_h. By means of the least square method the following correlation was derived

$$T^*_{max} = 1.71(Ra^* B/b)^{-0.220}(L/L_h)^{0.0365} \quad (9)$$

with $r^2 = 0.960$.

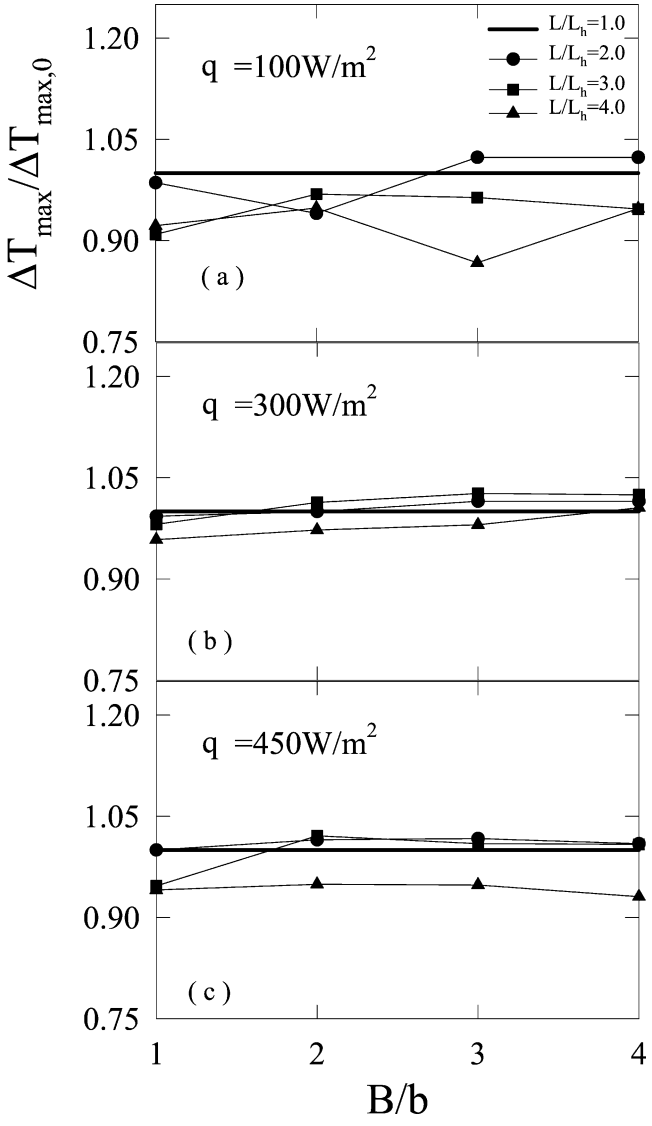

Fig. 7. Ratio of the maximum wall temperature rise above the ambient air in a channel with the adiabatic extension to the maximum wall temperature rise above the ambient air in a channel without the adiabatic extension vs the expansion ratio, for $L_h/b = 5.0$ and various L/L_h: (a) $q_\Omega = 100$ W·m^{-2}; (b) $q_\Omega = 300$ W·m^{-2}; (c) $q_\Omega = 450$ W·m^{-2}.

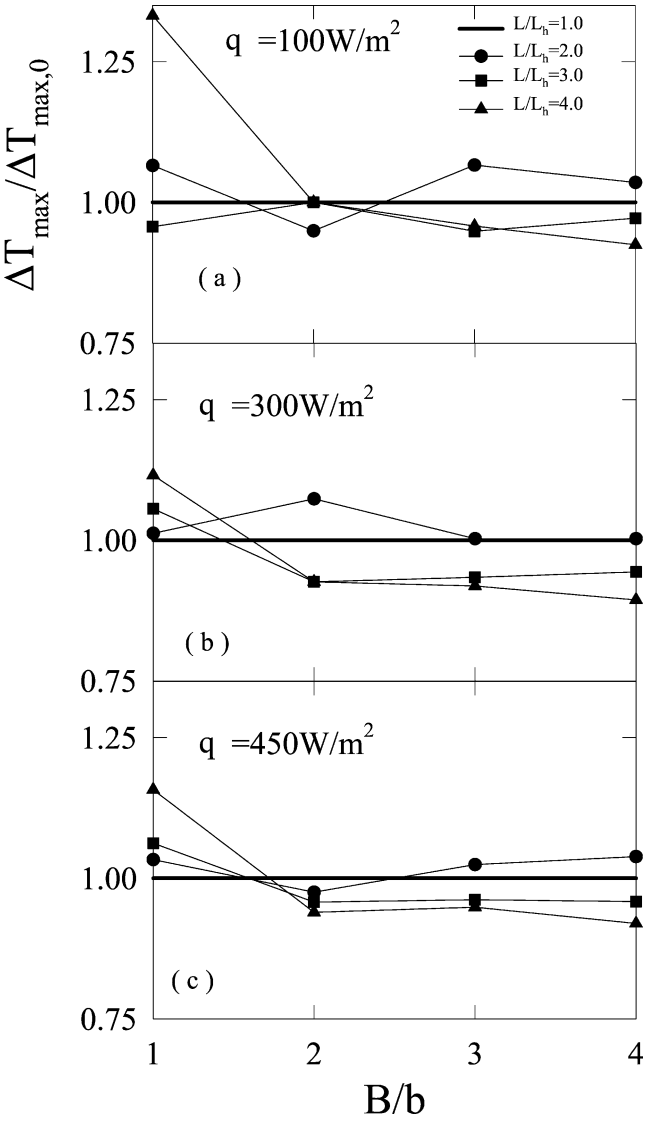

Fig. 8. Ratio of the maximum wall temperature rise above the ambient air in a channel with the adiabatic extension to the maximum wall temperature rise above the ambient air in a channel without the adiabatic extension vs the expansion ratio, for $L_h/b = 10.0$ and various L/L_h: (a) $q_\Omega = 100\ \mathrm{W\cdot m^{-2}}$; (b) $q_\Omega = 300\ \mathrm{W\cdot m^{-2}}$; (c) $q_\Omega = 450\ \mathrm{W\cdot m^{-2}}$.

Table 2
Coefficients in Eq. (10)

L/L_h	m'	n'	r^2
2.0	1.29	−0.170	0.940
3.0	1.25	−0.167	0.972
4.0	1.71	−0.208	0.961

Since 0.0365 is much smaller than 0.220, data were also correlated, for each value of $L/L_h = 2.0$, 3.0 and 4.0, by means of the equation

$$T^*_{max} = m'(Ra^* B/b)^{n'} \tag{10}$$

whose coefficients are reported in Table 2. Like it was expected, they are weakly dependent on the extension ratio and, therefore, all experimental data were correlated, in the same 10–1.5 × 10^5 range of $Ra^* \times B/b$, by the following equation, for all investigated values of L/L_h

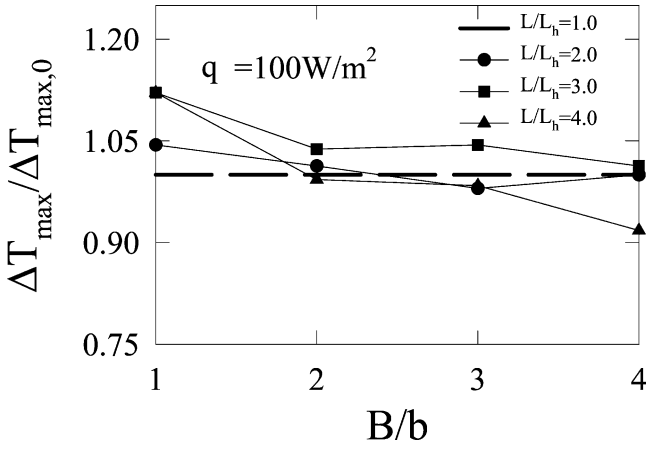

Fig. 9. Ratio of the maximum wall temperature rise above the ambient air in a channel with the adiabatic extension to the maximum wall temperature rise above the ambient air in a channel without the adiabatic extension vs the expansion ratio, for $L_h/b = 20.0$ and various L/L_h, $q_\Omega = 100\ \mathrm{W\cdot m^{-2}}$.

$$T^*_{max} = 1.40(Ra^* B/b)^{-0.178} \tag{11}$$

with $r^2 = 0.955$.

Experimental data and curves from Eq. (10) for $L/L_h = 4.0$ and from Eq. (11) for $L/L_h = 2.0$, 3.0 and 4.0 are reported in Fig. 10(a) and (b), respectively. Fig. 10(a) points out a weak dependence of T^*_{max} on $Ra^* \times B/b$ for $Ra^* \times B/b > 4.0$, that indicates a poor improvement in the thermal performance of the chimney-channel system at increasing values of $Ra^* B/b$. Similar observations can be made on the dependence of the maximum wall temperature on the abscissa in Fig. 10(b), which exhibits a good agreement between the data and the correlation, that does not take into account the different values of the extension ratio.

5.3. Correlations for channel Nusselt number

Again according to the analysis carried out by Straatman et al. [6], the channel Nusselt number was correlated to the channel Rayleigh number times the expansion ratio, in the 10–1.5 × 10^5 range of $Ra^* \times B/b$, and to the extension ratio, in the 2.0–4.0 range of L/L_h. By means of the least square method the following correlation was derived

$$Nu = 1.28(Ra^* B/b)^{1.07}(L/L_h)^{-0.0628} \tag{12}$$

with $r^2 = 0.960$.

Since 0.0698 is smaller than 1.07, it is worthwhile to correlate data also for each value of $L/L_h = 2.0$, 3.0 and 4.0 by means of the equation

$$Nu = m''(Ra^* B/b)^{n''} \tag{13}$$

whose coefficients are reported in Table 3. One can notice that also in this case they are weakly dependent on the extension ratio and, therefore, all experimental data were

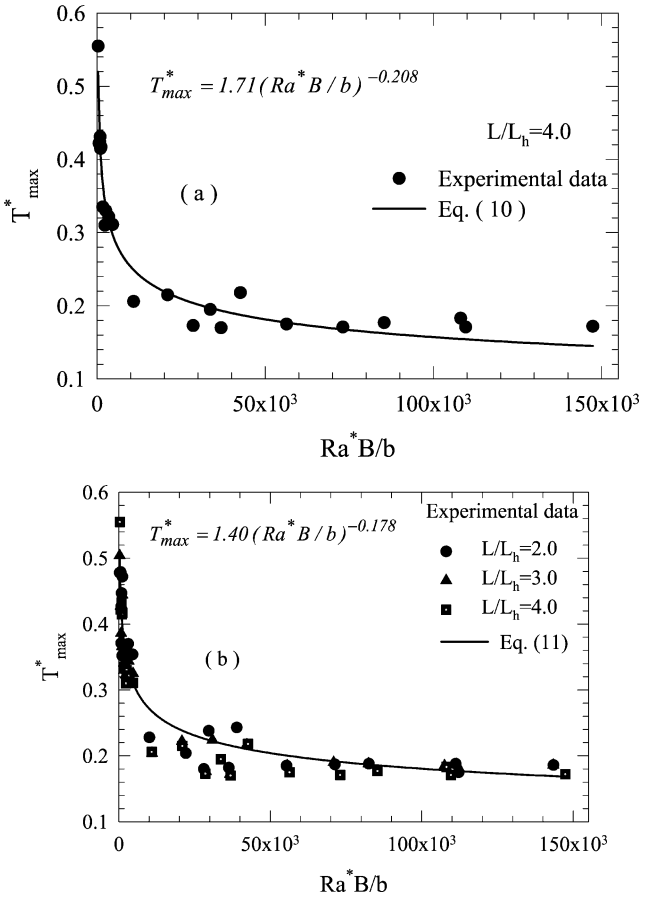

Fig. 10. Dimensionless maximum wall temperature vs the Rayleigh number times the expansion ratio: (a) $L/L_h = 4.0$; (b) $L/L_h = 2.0$, 3.0, 4.0.

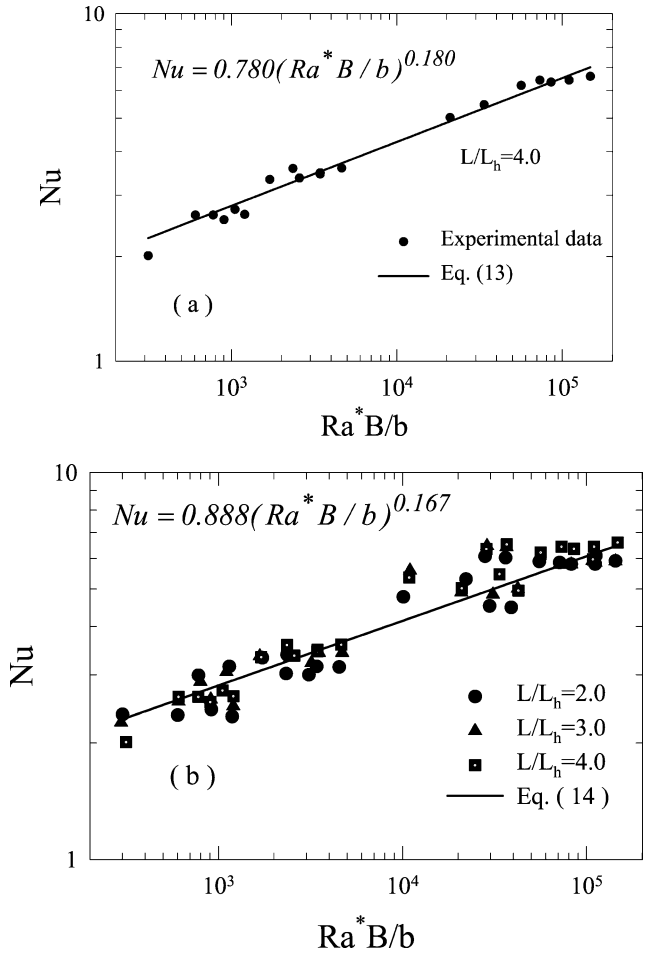

Fig. 11. Nusselt number vs the Rayleigh number times the expansion ratio: (a) $L/L_h = 4.0$; (b) $L/L_h = 2.0$, 3.0, 4.0.

Table 3
Coefficients in Eq. (13)

L/L_h	m''	n''	r^2
2.0	0.895	0.162	0.960
3.0	0.930	0.160	0.978
4.0	0.885	0.184	0.980

correlated, in the same 10–1.5×10^5 range of $Ra^* \times B/b$, by the following equation, for all investigated values of L/L_h

$$Nu = 0.888(Ra^* B/b)^{0.167} \quad (14)$$

with $r^2 = 0.960$.

Channel Nusselt numbers and the curves from Eq. (13) for $L/L_h = 4.0$ and from Eq. (14) for $L/L_h = 2.0$, 3.0 and 4.0 are reported in Fig. 11(a) and (b), respectively. The agreement between experimental data and the correlations can be considered good.

6. Conclusions

An experimental investigation on air natural convection in an asymmetrically heated vertical channel with unheated downstream extension was carried out. Results were obtained for different geometrical parameters and wall heat fluxes. Dimensionless maximum wall temperatures and Nusselt numbers were correlated to process parameters.

The addition of unheated extensions downstream of an asymmetrically heated vertical channel improved its thermal performance at both the heat fluxes under investigation for some configurations, the longer the extension the lower the wall temperature in the channel.

The larger the chimney the better the thermal performance of the system both in a large channel ($L_h/b = 5.0$) and in a channel-chimney system with a large ratio of the extension length to the channel length.

With a long extension ($L/L_h = 4.0$) the lower the aspect ratio the better the thermal performance of the system.

Dimensionless maximum wall temperatures and channel Nusselt numbers were correlated to the channel Rayleigh number times the expansion ratio, in the 10–1.5×10^5 range of $Ra^* \times B/b$, and to the extension ratio, in the 2.0–4.0 range of L/L_h. In the same ranges and for all values of the extension ratio, a single correlation for both dimensionless maximum wall temperature and channel Nusselt number was presented.

Acknowledgement

This research was supported by MIUR under the 2001 grant research program “Single Phase Natural and Mixed Convection: Fundamentals and Applications in Thermal Systems and Components”.

References

[1] G.P. Peterson, A. Ortega, Thermal control of electronic equipment and device, in: T.F. Irvine, J.P. Hartnett (Eds.), Advances in Heat Transfer, Vol. 2, Academic Press, New York, 1990, pp. 181–314.

[2] O. Manca, B. Morrone, S. Nardini, V. Naso, Natural convection in open channels, in: B. Sunden, G. Comini (Eds.), Computational Analysis on Convective Heat Transfer, WIT Press, Southampton, UK, 2000, pp. 235–278.

[3] W. Aung, L.S. Fletcher, V. Sernas, Developing laminar free convection between vertical plates with asymmetric heating, Internat. J. Heat Mass Transfer 15 (1972) 2293–2308.

[4] E.M. Sparrow, L.F. Azevedo, Vertical-channel natural convection spanning between the fully developed limit and the single-plate boundary layer limit, Internat. J. Heat Mass Transfer 28 (1985) 1847–1857.

[5] B.W. Webb, D.P. Hill, High Rayleigh number laminar natural convection in an asymmetrical heated vertical channel, J. Heat Transfer 111 (1989) 649–656.

[6] A.G. Straatman, J.D. Tarasuk, J.M. Floryan, Heat transfer enhancement from a vertical isothermal channel generated by the chimney effect, J. Heat Transfer 115 (1993) 395–402.

[7] A. Auletta, O. Manca, B. Morrone, V. Naso, Heat transfer enhancement by the chimney effect in a vertical isoflux channel, Internat. J. Heat Mass Transfer 44 (2001) 4345–4357.

[8] T.S. Fisher, K.E. Torrance, K.K. Sikka, Analysis and optimization of a natural draft heat sink system, IEEE Trans. Comp. Pack. A 20 (1997) 111–119.

[9] T.S. Fisher, K.E. Torrance, Free convection limits for pin-fin cooling, J. Heat Transfer 120 (1998) 633–640.

[10] T.S. Fisher, K.E. Torrance, Experiments on chimney-enhanced free convection, J. Heat Transfer 121 (1999) 607–608.

[11] W.W. Thrasher, T.S. Fisher, K.E. Torrance, Experiments on chimney-enhanced free convection from pin-fin heat sink, J. Electron. Pack. 122 (2000) 350–355.

[12] G.A. Ledezma, A. Bejan, Optimal geometric arrangement of staggered vertical plates in natural convection, J. Heat Transfer 119 (1997) 700–708.

[13] A. Bejan, Shape and Structure, from Engineering to Nature, Cambridge University Press, Cambridge, 2000.

[14] S.E. Haaland, E.M. Sparrow, Solutions for the channel plume and the parallel-walled chimney, Numer. Heat Transfer 6 (1983) 155–172.

[15] G.A. Shahin, J.M. Floryan, Heat transfer enhancement generated by the chimney effect in systems of vertical channel, J. Heat Transfer 121 (1999) 230–232.

[16] P.H. Oosthuizen, A numerical study of laminar free convective flow through a vertical open partially heated plane duct, ASME HTD 32 (1984) 41–48.

[17] K.T. Lee, Natural convection in vertical parallel plates with an unheated entry or unheated exit, Numer. Heat Transfer Appl. 25 (1994) 477–493.

[18] A. Campo, O. Manca, B. Morrone, Numerical analysis of partially heated vertical parallel plates in natural convective cooling, Numer. Heat Transfer Appl. 36 (1999) 129–151.

[19] Y. Asako, H. Nakamura, M. Faghri, Natural convection in a vertical heated tube attached to thermally insulated chimney of a different diameter, J. Heat Transfer 112 (1990) 790–793.

[20] S.J. Kline, F.A. McClintock, Describing uncertainty in single sample experiments, Mech. Engrg. 75 (1953) 3–12.

[21] R.J. Moffat, Describing the uncertainties in experimental results, Exp. Therm. Fluid Sci. 1 (1988) 3–17.